Beyond absorption maxima: the impact of wavelength-resolved photochemistry on materials science†

Quinten Thijssen, [ab] Joshua A. Carroll,[a] Florian Feist, [c] Andreas Beil, [d] Hansjörg Grützmacher, [d] Martin Wegener, [c] Sandra Van Vlierberghe [b] and Christopher Barner-Kowollik *[ac]

Reflecting on Giacomo Ciamician's revolutionary vision of harnessing sunlight to drive photochemical transformations, the field of materials science has evolved significantly, yet it has been constrained by the misconception that the highest reactivity in photochemical systems is achieved at the absorption maxima. Here, we explore this notion further with evidence from photochemical action plots, demonstrating that reactivity can indeed be maximal at wavelengths significantly separated from the absorption peak. By examining the implications of the disparity between absorptivity and photochemical reactivitiy, we explore its impact for the enhanced penetration depth of light in photoresists, the reduction of energy requirements for photochemical reactions, and its transformative potential for volumetric 3D printing. Ultimately, we argue for a renewed appreciation of light's capability to facilitate photochemical reactions across the entire volume of a material.

On the importance of light as a chemical tool

The vision of Giacomo Ciamician

Over a century has passed since the seminal publication by Italian photochemist Giacomo Ciamician, in which he shared his vision that was both revolutionary and prophetic:

"*On the arid lands there will spring up industrial colonies without smoke and without smokestacks; forests of glass tubes will extend over the plains and glass buildings will rise everywhere; inside of these will take place the photochemical processes that hitherto have been the guarded secret of the plants, but that will have been mastered by human industry which will know how to make them bear even more abundant fruit than nature, for nature is not in a hurry and mankind is. And if in a distant future the supply of coal becomes completely exhausted, civilization will not be checked by that, for life and civilization will continue as long as the sun shines!*"[1]

The question that looms large is whether we have managed to translate Ciamician's vision into tangible progress and how far we have ventured along the path he imagined. It is perhaps fair to state that while synthetic photochemistry has clearly had a dramatic impact not only on fundamental chemical research but also on the lives of every human being – from photovoltaic cells[2] to photodynamic therapy[3] to water purification[4] to dental materials[5] to 3D printed objects[6] – Ciamician's vision has not yet been fully realized. The reasons for this failure to translate are manifold, yet one reason stands taller than others in impeding the implementation of Ciamician's vision: when light penetrates a medium, it can be scattered, or trigger chemical processes with a certain quantum yield, and be absorbed. Thus, the penetration depth of light into matter is often limited, reducing the depth at which light – as a remarkable traceless reagent – can function, reinforcing the traditional view of light primarily as a surface phenomenon.[7]

In the current contribution, we will challenge this ingrained assumption based on wavelength-resolved photochemical data recorded over the last decade. We will demonstrate that the assumption that maximum absorptivity of light equals maximum chemical reactivity is invalid and – based on the latest

[a] *School of Chemistry and Physics, Queensland University of Technology (QUT), 2 George Street, Brisbane, QLD 4000, Australia. E-mail: christopher.barnerkowollik@qut.edu.au*

[b] *Polymer Chemistry and Biomaterials Group, Centre of Macromolecular Chemistry, Department of Organic and Macromolecular Chemistry, Ghent University, Krijgslaan 281, S4, 9000, Ghent, Belgium*

[c] *Institute of Nanotechnology (INT) and Institute of Applied Physics (APH), Karlsruhe Institute of Technology (KIT), Herrmann-von-Helmholtz-Platz 1, 76344 Eggenstein-Leopoldshafen, Germany*

[d] *Department of Chemistry and Applied Biosciences, ETH Zürich, Vladimir-Prelog-Weg 1, 8093 Zürich, Switzerland*

findings in the field of wavelength-resolved photochemistry – show that high reactivities and even maximum reactivities can be exploited at extremely low absorptions to conduct high penetration depth photochemistry with an immediate impact on materials science applications. We will argue in our Conclusion section that Ciamician's vision is perhaps closer to realization than we might believe, provided we induce photochemical processes guided by wavelength-resolved reactivity data.

Light as a surface phenomenon

A photochemical reaction involves the absorption of a photon that ultimately brings forth, with a well-defined probability, a chemical change within the photo-responsive moiety that can be expressed in the form of a fragmentation, a rearrangement, or any other form of chemical change. This seemingly simplistic and holistic view of a photochemical reaction is the result of the establishment of a series of photophysical laws.

In the 19th century, Grotthuss and Draper established the so-called first law of photochemistry, which states that light has to be absorbed in order for a photochemical reaction to take place.[8] In the 20th century, Stark and Einstein further refined the concept of absorption by introducing the photo-equivalence law, also referred to as the second law of photochemistry, which states that, at most, a single molecule can be directly excited, by absorption of a single photon.[9] While it might seem obvious that not every absorbed photon will be 100% effective at inducing the respective chemical change, the correlation between absorption and reactivity has been generally deemed appropriate, *i.e.*, if more photons are absorbed at a specific wavelength, the photochemical yield at that wavelength must be increased. This view is further exemplified by the following citation of Grotthuss in 1818: '*In my opinion, the bodies, independently on their chemical nature, should react most intensely to a color that in the natural state is opposed to its natural color, and the least in the contrary case*.'[8]

The correlation between light absorptivity and reactivity, deeply ingrained in the field of photochemistry, suggests that reactions should be performed at the wavelength of maximum absorption (λ_{max}) to optimize efficiency. This perspective has imposed several generally accepted limitations on the use of light in materials sciences such as limited penetration depth, limitations related to scaling up photochemical processes for industrial applications, limited selectivity and control, and limited energy efficiency. Moreover, the view of light as primarily a surface phenomenon has significantly shaped both the development of technologies and the conceptual framework within which researchers operate, as illustrated by the focus on the development of shallow photochemical reactor vessels, thin materials or coatings, and the development of layer-by-layer stereolithography.

Red-shifted reactivity and wavelength-resolved photochemistry

Light has long been present in traditional polymer or organic chemistry laboratories, typically in the form of medium or high-pressure mercury lamps, deuterium lamps, or fluorescent lamps, used to cure polymer films/coatings, perform photochemical reactions, conduct UV-vis analyses, develop thin layer chromatography plates, or serve as an add-on in a rheometer.

With the introduction of LEDs and laser systems in conventional chemical laboratories, characterized by a narrower wavelength distribution, a range of photochemical reactions were observed to exhibit significantly higher activity at conditions that could not be predicted based solely on conventional UV-vis spectroscopy. This effect was first observed by the teams of Barner-Kowollik and Gescheidt in 2017, when they recorded what is now considered the first modern-day photochemical action plot.[10]

The unexpected mismatch between photochemical reactivity and absorptivity challenges the long-standing assumption – well captured by the noted Grotthuss quote from 1818 above – that the peak of the efficiency of a photochemical reaction is directly correlated with the peak of optical absorption. The broad spectrum of traditional light sources such as mercury, deuterium, or fluorescent lamps often mask the critical influences of specific wavelengths on the photochemical activity, accompanied by the fact that most, if not all, photochemical systems are active at their respective absorption maxima.

To effectively assess the wavelength-resolved reactivity of a chemical system, it is imperative to determine the chemical conversion and/or yield in a wavelength-resolved manner. Such a wavelength-resolved analysis of the reactivity of a photochemical system is commonly reported as the above noted photochemical action plot.[11,12] Action plots can be obtained by delivering an identical number of photons for specific monochromatic wavelengths – by means of a wavelength-resolved laser system – and subsequent mapping of the chemical reactivity *via* chemical characterization techniques such as mass spectrometric and nuclear magnetic resonance spectroscopic techniques.

The mismatch between the peak of the efficiency of the photochemical reaction – which notably can also manifest as a blue-shift – has since been illustrated for a plethora of photochemical systems, including but not limited to, the [2+2] cycloaddition of styrylquinoxaline, dimerization of chalcone, photopolymerizations initiated by oxime esters, the dimerization of pyrene-chalcone, and photo-triggered ATRP of poly(meth)acrylates.[10 17] We note that the purpose of the current contribution is not to explore the underlying causes of the mismatch between absorptivity and wavelength resolved reactivity, which can include complex excited state dynamics, influences due to the microenvironment around chromophores,[18] and complex reaction kinetics induced by competing absorption as well as a combination of these causes. These have been discussed elsewhere and will continue to be explored.[12]

The impact of wavelength-resolved photochemistry on materials science

The introduction of wavelength-resolved photochemistry to materials science calls for a re-evaluation of previously accepted limitations of the use of photochemical systems in materials science, which will be discussed in the following section.

Influence on the penetration depth of light

To illustrate the influence of red-shifted reactivity on penetration depth, it is imperative to first consider how the intensity of

light reduces as it traverses a medium. The reduction in light intensity is quantified by the extinction coefficient α_{ext}, expressed in units of inverse length, which contains both the absorption and scattering contributions:

$$\alpha_{ext} = \alpha_{abs} + \alpha_{sca} = N(C_{abs} + C_{sca}) \quad (1)$$

Here, α_{abs} and α_{sca} represent the absorption and scattering coefficients, C_{abs} and C_{sca} represent the absorption and scattering cross sections, and N represents the number density of molecules. The absorption cross-section C_{abs} can be further related to the molar absorption coefficient ε_{abs} and the molar concentration c. Specifically, C_{abs} can be written as:

$$C_{abs} = \frac{\varepsilon_{abs}\ln 10}{N_A} = \frac{\varepsilon_{abs} c \ln 10}{N} \quad (2)$$

On the other hand, the scattering cross-section C_{sca} can be approximated for small molecules by integrating the Rayleigh scattering intensity equation over all scattering angles. The Rayleigh scattering differential cross-section is given by:[19]

$$I_{sca} = I_{source}\frac{(2\pi)^4}{\lambda^4} r^6 \left(\frac{n^2-1}{n^2+2}\right)^2 \frac{1}{2}(1+\cos^2\theta) \quad (3)$$

Here, I refers to the intensity, r refers to the particle radius, n represents the refractive index, λ refers to the wavelength of the incident light, and ϑ to the scatter angle. Integrating this over all angles results in the total scattering cross-section for small spherical particles:

$$C_{sca} = \frac{8\pi(2\pi)^4}{3\lambda^4} r^6 \left(\frac{n^2-1}{n^2+2}\right)^2 \quad (4)$$

Thus, the extinction coefficient combining both absorption and scattering contributions can be related to the initial intensity I_i and the intensity I_t after traveling the distance d in the medium as follows:

$$\frac{I_t}{I_i} = e^{(-\alpha_{ext} d)} = e^{\left(\varepsilon_{abs} c \ln 10 + N\frac{8\pi(2\pi)^4}{3\lambda^4} r^6 \left(\frac{n^2-1}{n^2+2}\right)^2\right) d} \quad (5)$$

Conversely, chemists and spectroscopists typically define the absorption of light that penetrates an absorbing non-scattering medium by the absorbance, which is determined using the common logarithm (base 10):

$$A = \log_{10}\frac{I_t}{I_i} = \varepsilon_{abs} c d = \alpha_{abs,10} d \quad (6)$$

As a result, the absorption coefficient α_{abs}, used throughout the current contribution, is related to the decadic absorption coefficient $\alpha_{abs,10}$ as follows:

$$\alpha_{abs} = \alpha_{abs,10}\ln(10) = \varepsilon_{abs} c \ln(10) \quad (7)$$

With these theoretical underpinnings in mind, extinction encompasses both the absorption of photons by a material and their scattering within the medium, recorded as a decrease in transmission through the sample. Consequently, the correlation between UV-vis spectroscopy in transmission and absorption is only valid when the scattering contribution is negligible. In most diluted solutions, the difference between the absorption and extinction spectrum is minor. However, when considering the interactions of light with solutions in which crosslinked polymer networks are being formed, as encountered in 3D printing, scattering needs to be considered. In the following, we will briefly discuss the influence of scattering on a general level.

Scattered light originates from the oscillations of induced dipole moments of a molecule by an incident light wave.[20] When the size of particles is much smaller than the wavelength of the incident light, with concentrations sufficiently low to ignore intermolecular interactions/multiple scattering events, and particles are also approximately spherical in shape, the scattering can be simply modelled by the Rayleigh scattering approximation shown by eqn (3),[20] with a scattering intensity dependence on incident wavelength that follows λ^{-4}.

This situation is the case for the vast majority of typical UV-vis spectroscopy measurements with low chromophore concentrations (such that intermolecular interactions and multiple scattering events are minimal) and in the absence of substantial aggregation. Under such conditions, contributions from scatter are small and follow λ^{-4}. However, as particle/molecule sizes approach the wavelength of incident light, or their shape is no longer approximately spherical – *e.g.* proteins or large polymers – the approximation becomes less applicable and the divergence between extinction and absorption becomes more pronounced. In such cases, scattering is no longer isotropic and the overall magnitude of scatter increases. Typically, the impact due to size will be minimal for polymer chains freely dissolved in solution, as the polymer size to wavelength ratio is often <0.1. However, non-spherical shapes of polymer chains can result in the Rayleigh approximation underestimating the degree of scatter. Here, more rigorous models that take particle shape into account, such as advanced Mie scattering, or experimental techniques such as static light scattering, are required to accurately determine scattering contributions. Thus, for the photochemical formation of crosslinked polymer networks – a process that so far has not been probed by action plots to the best of our knowledge – the question of scattering must be further considered as both the size and the local concentration of polymer networks becomes significant. In addition to scattering scenarios where more advanced scattering models are required, it is important to consider that scattered photons can also be absorbed, adding another layer of complexity to the interaction of light with the scattering medium. However, this is considered beyond the scope of the current article. Yet, it should be noted that, red-shifting the wavelength of irradiation can be exploited to reduce the scattering contribution.

Keeping this nuanced understanding of the correlation between UV-vis spectra and absorption in mind, it is informative to consider how the number of photons at a specific wavelength decreases as a function of penetration depth, as illustrated in Fig. 1. In photochemical systems characterized by an absorption coefficient above 1 cm^{-1}, 99% of the initial photon amount is absorbed within a penetration depth of 4.6 cm. Typical photochemical systems exhibit absorption

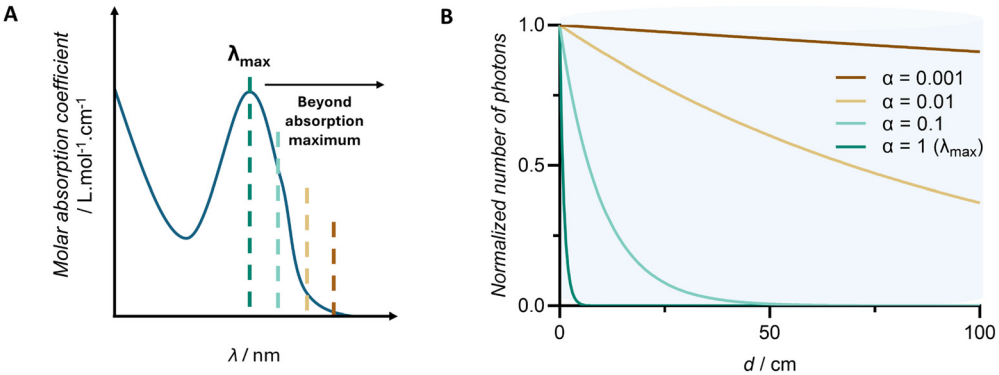

Fig. 1 Illustration of how red-shifting the wavelength of irradiation beyond the absorption maximum (panel A) leads to a significant increase in the penetration depth of the irradiation in a volume of photoresist, illustrated by the number of photons as a function of penetration depth across a range of absorption coefficients from 1 to 0.001 (panel B). The normalized number of photons at any depth is the intensity at that depth divided by the initial intensity, which follows an exponential decay according to the Lambert–Beer law as presented in Section 2 of the ESI.†

coefficients well above 1 cm $^{-1}$, often exceeding 100 cm $^{-1}$. In such cases, 99% of the incident photons are absorbed within the first 461 μm, reinforcing the traditional view of light as primarily a surface phenomenon. However, this perception shifts significantly when photochemical systems with absorption coefficients of 0.1 and 0.01 cm $^{-1}$ are considered, as for these systems, 99% of the incident photons are absorbed only after penetration depths of 0.46, 4.6 meters, respectively. Intriguingly, due to the red-shifted reactivity (*i.e.*, the phenomenon of observing the peak chemical reactivity at wavelengths of light that are red-shifted relative to the absorption maximum), absorption coefficients in the range of 0.1 to 0.01 cm $^{-1}$ become practical, demonstrating that photochemical systems can effect change throughout the entire volume of material, potentially covering multiple cubic meters.

Having outlined the physical underpinnings of light interactions with reaction solutions, let us now examine two practical examples that demonstrate how photochemical action plots can be strategically used to design systems with significant penetration depths: the photopolymerization of methyl methacrylate (MMA) using ^{Mes}BAPO-NH$_2$ as photo-initiator, and the photo-crosslinking of a polymeric precursor by means of a photodimerization reaction.

First, let us consider the design of a photoresist based on the light-initiated free-radical polymerization of methyl methacrylate using ^{Mes}BAPO-NH$_2$ as a photo-initiator to give poly(methyl methacrylate) (PMMA). To inform this design, a photochemical action plot was recorded by delivering an equal number of photons at various wavelengths, followed by gravimetric determination of the conversion of methyl methacrylate, as illustrated in Fig. 2. It should be noted that the respective photochemical action plot does not directly provide information related to the quantum yield at each wavelength for the fragmentation of the photo-initiator; instead, it quantifies the effective monomer conversion, encapsulating 'the sum of all effects' of the photopolymerization system that may contribute to the shape of the action plot under the specific employed reaction conditions. Moreover, it is important to recognize that in photo-initiated polymerizations—typically 'cascade reactions'—high quantum yields are common, with a single photon potentially triggering a chain reaction that can yield a polymer incorporating more than 100 monomer units.

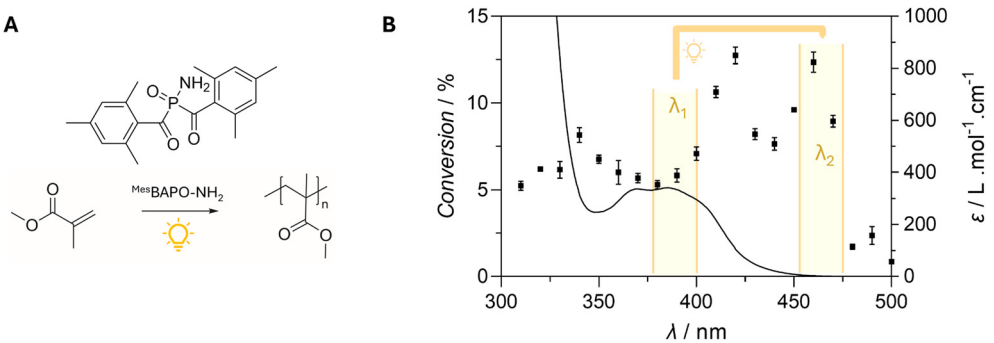

Fig. 2 (A) Photopolymerization of methyl methacrylate (MMA) initiated by the photo-initiator ^{Mes}BAPO-NH$_2$ (c_{PI} = 5 mmol L^{-1}), (B) photochemical action plot of the photopolymerization illustrating that the monomer conversion is higher in a wavelength regime where the absorption is very low. The yellow arrow indicates that the highest reactivities can be obtained at the far red-edge, where the extinction is minimal, thus offering a key opportunity for deep penetration with high reactivities. Solutions were irradiated with 6.02 × 10^{19} photons at each wavelength. Refer to the first and third section of the ESI† for the calculations related to the provided example and the experimental data related to the recording of the photochemical action plot, respectively.

Therefore, such systems are particularly well-suited for volumetric applications.

Based on the photochemical action plot, a (meth)acrylate-based photoresist can be designed for applications that require deep light penetration. The proposed example utilizes a concentration of 0.5 wt% ^{Mes}BAPO-NH$_2$, a concentration commonly employed in photopolymerizable formulations (*i.e.*, 0.014 M – assuming a density of 1 g cm ^{3} and a molar mass of 357 g mol ^{1}) and considers a photoresist in which 99% of incident photons are absorbed only beyond a penetration depth of 2 m (corresponding to an absorption coefficient of 0.023 cm ^{1}). The respective concentration and absorption coefficient limit the molar absorption coefficient to 0.713 L mol ^{1} cm ^{1} in order to achieve the desired penetration depth. Interestingly, the photochemical action plot reveals that at 470 nm—a wavelength substantially red-shifted by 80 nm from the peak absorption—the system maintains high reactivity while adhering to this molar absorption constraint. Thus, this specific choice of wavelength, driven by the need to limit the molar absorption coefficient, highlights the critical role of the photochemical action plot. It ensures that high reactivity is maintained under conditions necessary for deep penetration, a complex interplay of factors that UV-vis spectroscopy alone cannot predict. Conversely, had the design relied solely on UV-Vis spectroscopy, the selection of an irradiation wavelength at 385 nm, where the molar absorption coefficient peaks at 341 L mol ^{1} cm ^{1}, would result in 99% of the photons being absorbed within just 4.18 mm.

Another illustrative example is provided by the design of a photoresist employing non-radical photochemical reactions, designed to achieve substantial penetration depths. Such a design is pivotal for applications such as volumetric 3D printing (*vide infra*), a field where non-radical photochemical reactions have yet to be introduced. The central design challenge lies in determining the optimal chromophore concentration that balances desired penetration depth with maintained high reactivity, guiding the selection of an appropriate structure and molar mass for the polymeric precursor. Consider a photoresist based on the photo-dimerization of styrylpyrene, where 99% of the incident photons are absorbed only beyond a penetration depth of 2 meters (again corresponding to an absorption coefficient of 0.023 cm ^{1}). Based on the photochemical action plot, illustrated in Fig. 3, one can infer that at a wavelength of 450 nm, where the molar absorption coefficient is 85 L mol ^{1} cm ^{1}, the net photodimerization reaction demonstrates high reactivity. With these parameters, the chromophore concentration can be set at 1.2 × 10 ^{4} mol L ^{1}. Thus, to ensure effective network formation and maintain the envisioned high penetration depth, one would synthesize a trifunctional star-shaped polymer with a molar mass of 25 000 g mol ^{1}, end-functionalized with styrylpyrene at the respective chain ends. It should be noted that the described example assumes a pristine polymer system devoid of any solvent or additive, and a density of 1 g cm ^{3}. Conversely, a UV-vis spectroscopic inspection of the absorption spectrum of the monomer would fail to predict the high reactivity at a wavelength of 450 nm and, even at the lower end of the absorption spectrum, the molar absorption coefficients exceed the levels conducive for the required penetration depth, rendering such a design impossible solely relying on UV-vis spectroscopy.

The aforementioned examples illustrate the potential of wavelength-resolved photochemistry and the utility of photochemical action plots in extending the application of photochemical systems beyond applications with limited penetration depth. This advancement paves the way for the application of light in volumetric systems, where light is expected to induce chemical changes throughout the entire volume of the material. It should be noted that the reasons for the observed mismatch between absorptivity and reactivity can be complex and each system has to be examined on its own merits. We refer the reader to a recent overview discussion.[12]

Influence on the photochemical energy cost

The concept of red-shifted reactivity and its influence on energy requirements in materials science presents another interesting aspect. Starting with the premise that an equal number of photons from two different wavelengths, *X* (higher photon energy) and *Y* (red-shifted, thus lower photon energy), can be employed to induce the same chemical change within a photochemical system (*i.e.*, equal quantum yields are assumed),

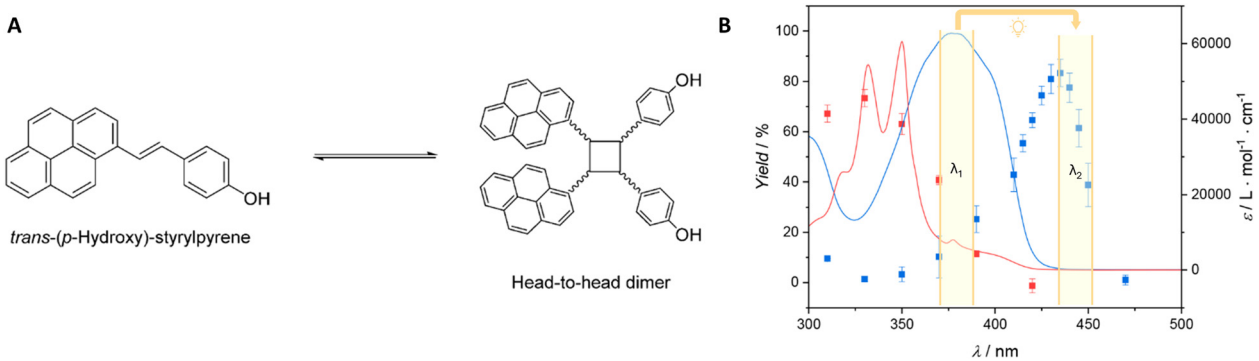

Fig. 3 (A) Photochemically reversible [2+2] cycloaddition of *trans*-(*p*-hydroxy)styrylpyrene. For the sake of simplicity, only the head-to-head dimer is shown. (B) Photochemical action plot of the dimerization (in blue) and the dissociation (in red) of *trans*-(*p*-hydroxy)styrylpyrene. The highlighted yellow area illustrates the red-shifted reactivity to wavelength regimes where absorption is significantly lower. Adjusted from ref. 17.

allows for an evaluation of their respective influence on the required energy.

To illustrate the concept, consider the energy of a photon given by eqn (8), where E is the photon energy, h is Planck's constant ($6.626t \times 10^{-34}$ J s), c is the speed of light in a vacuum (2.99×10^{8} m s^{-1}), and λ is the wavelength.

$$E = \frac{hc}{\lambda} \tag{8}$$

For simplicity, consider a photochemical system for which identical photochemical reactivity is observed (*i.e.*, equal quantum yield) at two distinct wavelengths that represent a possible shift in reactivity: 360 and 420 nm. The energy for each photon in a vacuum at both wavelengths can be calculated as 5.5×10^{-19} J and 4.7×10^{-19} J. As a practical example, consider the photochemical synthesis of one ton of a photochemical product with a molar mass of 250 g mol^{-1} and a quantum yield of 0.1. Hereto, the total number of photons required can be calculated to be 2.4×10^{28}, which corresponds to 13.3×10^{9} J and 11.4×10^{9} J for 360 nm and 420 nm photons, respectively.

The energy savings of 1.9 billion joules, or more commonly referred to as 527.8 kW h, for producing one ton of product can significantly contribute to scaling up photochemical reactions for industrial applications, especially when considering that much larger production volumes can be addressed simultaneously. On the other hand, much less dilute conditions can be employed, thereby reducing solvent consumption, rendering the respective photochemical system more environmentally friendly.

However, it should be noted that the proposed calculations represent an oversimplification of reality, and it is critical to recognize that many additional factors must be considered for a comprehensive assessment. Key factors include the quantum yield at specific wavelengths—which may significantly vary as a function of wavelength—as well as the energy efficiency and achievable power of the irradiation source at specific wavelengths, among others.[21]

Despite these simplifications, the individualized assessment of industrial photochemical systems, informed by photochemical action plots, offers substantial potential to enhance throughput and minimize environmental impact.

A practical example: volumetric 3D printing

Volumetric 3D printing (VP) is revolutionizing the fabrication of complex three-dimensional objects and stands as a prime example of utilizing light to induce change across an entire volume of photoresist, illustrating the profound potential of understanding light as a three-dimensional and spatially resolved tool.[6] While the focus of the following discussion will be on tomographic volumetric 3D printing, it is important to note that other emerging volumetric 3D printing approaches (defined here as 3D-printing processes where photopolymerization occurs within the volume of the photoresist rather than at the surface), such as step-wise multi-photon-based approaches (*i.e.*, light-sheet printing),[22–26] also heavily rely on having a sufficiently large penetration of light in the photoresist.

Tomographic VP constructs objects by projecting a set of 2D images from different angles into a photopolymerizable resin, with the object being created in locations where the cumulative three-dimensional light dose distribution exceeds a certain critical light dose, as illustrated in Fig. 4A.[27–30] High photo-initiator concentrations ensure high reactivity and a large dose contrast between in-part and out-of-part voxels, while low photo-initiator concentrations ensure a homogeneous intensity profile and large penetration depth of the incident irradiation. This fundamental trade-off between achieving deep and homogeneous light penetration while ensuring sufficient reactivity within the photoresist imposes the choice between 3D objects that are either high resolution or large volume.

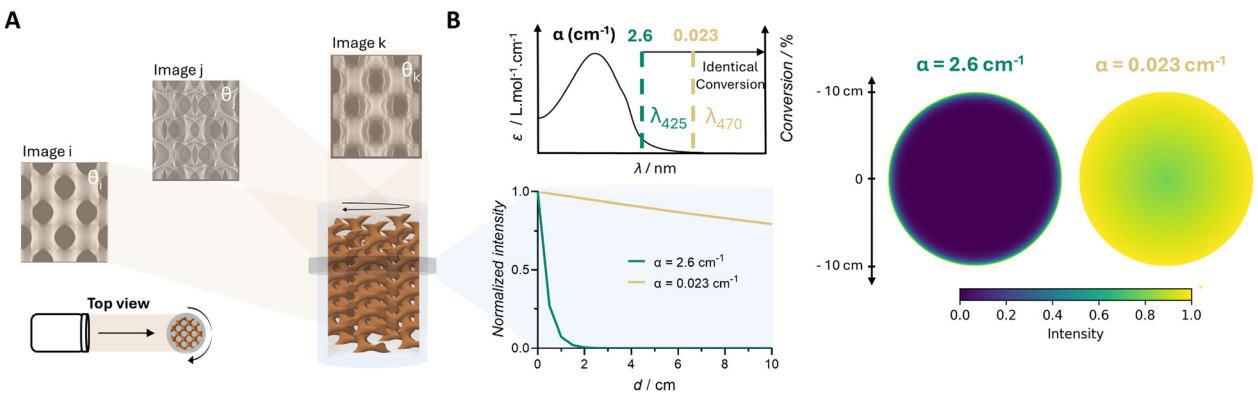

Fig. 4 (A) Shows a schematic depiction of volumetric 3D printing where a set of projections is delivered to a rotating volume of photoresist. (B) Illustrates a practical example how red-shifting the irradiation wavelength beyond the absorption maximum can improve penetration depth and uniformity of the light dose in tomographic volumetric 3D printing, based on the photopolymerization a (meth)acrylate-based resist, as illustrated in Fig. 2. By red-shifting the wavelength of irradiation from 425 to 470 nm, the absorption coefficient can be varied from 2.6 to 0.023 cm^{-1}. On the right side of panel B, the top view of the cylindrical photoresist is shown, with the light intensity profile described by the Bouguer-Lambert–Beer law for absorption coefficients of 2.6 cm^{-1} and 0.023 cm^{-1}. The center exhibits the lowest intensity because the vial is rotating and the irradiation source is positioned outside the photoresist. Detailed calculations for this intensity profile are provided in Section 2 of the ESI.†

Red-shifting the wavelength of irradiation beyond the absorption maxima, guided by a photochemical action plot, is projected to help achieve this delicate balance by reducing light absorption and scattering, allowing for deeper light penetration and more uniform light distribution within the photoresist, while high reactivity is maintained. In the context of VP, the insights from photochemical action plots and wavelength-resolved photochemistry are particularly valuable since they can be used to identify regions where the reactivity remains high but where the absorption coefficient is lower. By leveraging the ability to achieve high reactivity at red-shifted wavelengths, the limitations traditionally imposed by the absorption maximum can be overcome. This not only enhances the penetration depth and uniformity of light within the photoresist but also supports the creation of larger and more precise 3D objects.

While in the field of volumetric 3D printing, it is common to irradiate off-peak to reduce attenuation throughout the photoresist, the information obtained by the action plot enables one to identify exactly how far beyond the peak of maximal absorption can be irradiated without loss of chemical reactivity.[6] For example, in case of the free-radical photopolymerization of methyl methacrylate (MMA), which was discussed earlier, it was demonstrated that by red-shifting the wavelength of irradiation by 80 nm, with respect to the absorption maximum, to 470 nm, the molar absorption coefficient can be reduced to 0.713 L mol $^{-1}$ cm $^{-1}$ while high reactivity is maintained. Thus, when the photoresist is irradiated with 470 nm light, and a photo-initiator concentration of 0.5 wt% is assumed, the absorption coefficient corresponds to 0.023 cm $^{-1}$. In contrast, when the same photo-initiator concentration is considered, irradiation at the tail end of the UV-Vis spectrum at 425 nm results in a molar absorption coefficient of 80 L mol $^{-1}$ cm $^{-1}$, corresponding to an absorption coefficient of 2.6 cm $^{-1}$. Here it should be noted that, while we base our example on the system provided in Fig. 2, this system would need to be altered to involve a multifunctional monomer for its practical application to volumetric 3D printing.

In Fig. 4B, the influence on the light intensity profile across the photoresist of this respective shift from an absorption coefficient of 2.6 cm $^{-1}$ to 0.023 cm $^{-1}$ is illustrated. It is important to note that an absorption coefficient of 2.6 cm $^{-1}$ aligns with the typical size of objects produced *via* VP, which range between 0.4 and 1 cm in diameter, with the largest construct reported to date having an approximate diameter of 4 cm, albeit at very low resolution.[28] However, Fig. 4B clearly shows that introducing wavelength-resolved photochemistry into the field of volumetric 3D printing can not only provide a much more homogeneous light intensity distribution, improving the resolution and accuracy of VP, but can also do so at practically achievable dimensions as large as 20 cm in diameter. This illustrates that the implementation of photochemical action plots and wavelength-resolved photochemistry holds great potential for advancing the precision and throughput of VP.

Overarching implications for materials science

Reflecting on Giacomo Ciamician's vision, the journey from conceptualizing light to exploring it as a volumetric tool in materials science has shown significant progress. The discovery of mismatched reactivity in regions of low absorptivity, along with its concomitant implications for penetration depth and energy efficiency, warrants a re-evaluation of the generally accepted limitations of photochemical systems.

Practical examples for exploiting shifted reactivity are abundant, contributing to a sustainable future by implementing photo-triggered dynamic covalent chemistries that can be activated throughout the bulk of a much larger volume of material. In the biomedical field, red-shifted reactivity enables the generation of homogeneous drug-delivery vehicles that can release drugs upon irradiation at significantly greater penetration depths or facilitate deeper activation of injectable photoresponsive hydrogels, enhancing therapeutic outcomes. The manufacturing of objects through volumetric 3D printing can achieve unprecedented accuracy and construct sizes that are orders of magnitude larger than what is currently possible. In material sciences, applications such as coatings and surface treatments can benefit from deeper penetration of light, resulting in more uniform curing. Bulk polymerizations can achieve more uniform properties throughout large-scale materials due to improved light penetration. Even in fields such as robotics and bioelectronics, light can be exploited to effectuate changes over much larger penetration depths, enabling the development of more advanced and responsive materials. Furthermore, red-shifted reactivity can be harnessed to effectively use sunlight, thereby increasing the throughput and sustainability of photochemical synthesis.

The aforementioned examples not only rejuvenate Ciamician's dream but amplify the call for the introduction of wavelength-resolved photochemistry in the field of materials science.

Author contributions

The article was written with contributions from all authors.

Conflicts of interest

There are no conflicts to declare.

Acknowledgements

Q. T. acknowledges the Research Foundation – Flanders for a PhD (FWO-SB) and a junior postdoctoral fellowship with grant

numbers 1SA2323N and 1201125N. S. V. V. acknowledges the Research Foundation – Flanders for providing a Hercules grant (I003922N). C. B.-K. acknowledges the Australian Research Council (ARC) for a Laureate Fellowship. C. B.-K. and M. W. acknowledges key funding by the Deutsche Forschungsgemeinschaft (DFG, German Research Foundation) under Germany's Excellence Strategy for the Excellence Cluster ''3D Matter Made to Order'' (EXC-2082/1-390761711), by the Carl Zeiss Foundation, and by the Helmholtz program ''Materials Systems Engineering''.

Notes and references

1 G. Ciamician, *Science*, 1912, **36**, 385–394.
2 B. O'Regan and M. Grätzel, *Nature*, 1991, **353**, 737–740.
3 I. O. L. Bacellar, T. M. Tsubone, C. Pavani and M. S. Baptista, *Int. J. Mol. Sci.*, 2015, **16**, 20523–20559.
4 N. Corrigan, J. Yeow, P. Judzewitsch, J. Xu and C. Boyer, *Angew. Chem., Int. Ed.*, 2019, **58**, 5170–5189.
5 J. W. Stansbury and M. J. Idacavage, *Dent. Mater.*, 2016, **32**, 54–64.
6 Q. Thijssen, J. Toombs, C. C. Li, H. Taylor and S. Van Vlierberghe, *Prog. Polym. Sci.*, 2023, **147**, 101755.
7 L. Finlayson, I. R. M. Barnard, L. McMillan, S. H. Ibbotson, C. T. A. Brown, E. Eadie and K. Wood, *Photochem. Photobiol.*, 2022, **98**, 974–981.
8 A. Albini, *Photochem. Photobiol. Sci.*, 2016, **15**, 319–324.
9 A. Einstein, *Ann. Phys.*, 1905, **322**, 132–148.
10 D. E. Fast, A. Lauer, J. P. Menzel, A.-M. Kelterer, G. Gescheidt and C. Barner-Kowollik, *Macromolecules*, 2017, **50**, 1815–1823.
11 I. M. Irshadeen, S. L. Walden, M. Wegener, V. X. Truong, H. Frisch, J. P. Blinco and C. Barner-Kowollik, *J. Am. Chem. Soc.*, 2021, **143**, 21113–21126.
12 S. L. Walden, J. A. Carroll, A.-N. Unterreiner and C. Barner-Kowollik, *Adv. Sci.*, 2024, **11**, 2306014.
13 K. Kalayci, H. Frisch, V. X. Truong and C. Barner-Kowollik, *Nat. Commun.*, 2020, **11**, 4193.
14 I. M. Irshadeen, K. D. Bruycker, A. S. Micallef, S. L. Walden, H. Frisch and C. Barner-Kowollik, *Polym. Chem.*, 2021, **12**, 4903–4909.
15 J. A. Carroll, F. Pashley-Johnson, H. Frisch and C. Barner-Kowollik, *Chem. – Eur. J.*, 2024, **30**, e202304174.
16 C. Ma, T. Han, S. Efstathiou, A. Marathianos, H. A. Houck and D. M. Haddleton, *Macromolecules*, 2022, **55**, 9908–9917.
17 R. T. Michenfelder, F. Pashley-Johnson, V. Guschin, L. Delafresnaye, V. X. Truong, H.-A. Wagenknecht and C. Barner-Kowollik, *Adv. Sci.*, 2024, 2402011.
18 A. P. Demchenko, *Luminescence*, 2002, **17**, 19–42.
19 J. D. Jackson, *Classical Electrodyn*, 3rd edn, 1998.
20 C. F. Bohren and D. R. Huffman, *Absorption and Scattering of Light by Small Particles*, John Wiley & Sons, 2008.
21 G. Goti, K. Manal, J. Sivaguru and L. Dell'Amico, *Nat. Chem.*, 2024, **16**, 684–692.
22 V. Hahn, F. Mayer, M. Thiel and M. Wegener, Optics & Photonics News - 3-D Laser Nanoprinting, **https://www.optica-opn.org/home/articles/volume_30/october_2019/features/3-d_laser_nanoprinting/**.
23 V. Hahn, P. Rietz, F. Hermann, P. Müller, C. Barner-Kowollik, T. Schlöder, W. Wenzel, E. Blasco and M. Wegener, *Nat. Photonics*, 2022, **16**, 784–791.
24 M. Regehly, Y. Garmshausen, M. Reuter, N. F. König, E. Israel, D. P. Kelly, C. Y. Chou, K. Koch, B. Asfari and S. Hecht, *Nature*, 2020, **588**, 620–624.
25 V. Hahn, P. Rietz, F. Hermann, P. Müller, C. Barner-Kowollik, T. Schlöder, W. Wenzel, E. Blasco and M. Wegener, *Nat. Photonics*, 2022, 1–8.
26 V. Hahn, T. Messer, N. Maximilian Bojanowski, E. R. Curticean, I. Wacker, R. R. Schröder, E. Blasco and M. Wegener, *Nat. Photonics*, 2021, **15**, 932–938.
27 B. E. Kelly, I. Bhattacharya, M. Shusteff, H. K. Taylor and C. M. Spadaccini, *Proceedings of the 28th Annual International Solid Freeform Fabrication Symposium*, 2017, pp. 938–950.
28 B. E. Kelly, I. Bhattacharya, H. Heidari, M. Shusteff, C. M. Spadaccini and H. K. Taylor, *Science*, 2019, **363**, 1075–1079.
29 Q. Thijssen, A. Quaak, J. Toombs, E. De Vlieghere, L. Parmentier, H. Taylor and S. Van Vlierberghe, *Adv. Mater.*, 2023, **35**, 2210136.
30 D. Loterie, P. Delrot and C. Moser, *Nat. Commun.*, 2020, **11**, 1–6.